Available online at www.sciencedirect.com

ScienceDirect

www.elsevier.com/locate/jes

JES JOURNAL OF ENVIRONMENTAL SCIENCES

www.jesc.ac.cn

Research Article

Prediction model on hydrolysis kinetics of phthalate monoester: A density functional theory study

Tong Xu[1,2], *Jingwen Chen*[2,*], *Deming Xia*[2], *Weihao Tang*[2,3], *Jiansheng Cui*[1], *Chun Liu*[1], *Shuangjiang Li*[1]

[1] *College of Environmental Science and Engineering, Hebei University of Science and Technology, Shijiazhuang 050000, China*

[2] *Key Laboratory of Industrial Ecology and Environmental Engineering (Ministry of Education), School of Environmental Science and Technology, Dalian University of Technology, Dalian 116024, China*

[3] *National-Regional Joint Engineering Research Center for Soil Pollution Control and Remediation in South China, Guangdong Key Laboratory of Integrated Agro-environmental Pollution Control and Management, Institute of Eco-environmental and Soil Sciences, Guangdong Academy of Sciences, Guangzhou 510650, China*

ARTICLE INFO

Article history:
Received 29 September 2022
Revised 5 December 2022
Accepted 11 December 2022
Available online 17 December 2022

Keywords:
Phthalate monoesters
Phthalate esters
Hydrolysis
Density functional theory
Quantitative structure-activity relationship

ABSTRACT

As primary degradation products of phthalate esters, phthalate monoesters (MPEs) have been widely detected in various aquatic environments and drawn growing toxicological concerns. Hydrolysis kinetics that is of importance for assessing environmental persistence of chemicals remain elusive for MPEs. Herein, kinetics of base-catalyzed and neutral hydrolysis for 18 MPEs with different leaving groups was investigated by density functional theory calculation. Results indicate that MPEs with leaving groups having pK_a of <10 prefer dissociative transition states. MPEs are more persistent than their parents, and their hydrolysis half-lives were calculated to vary from 3.4 min to 79.2 years (pH = 7–9). A quantitative structure-activity relationship model was developed for predicting the hydrolysis kinetics parameters. It was found that pK_a of the leaving groups and electronegativity of the MPEs are key factors determining the hydrolysis kinetics. This work may lay a theoretical foundation for better understanding the chemical process that governs MPE persistence in aquatic environments.

Introduction

Phthalate monoesters (MPEs) are generated from primary degradation of phthalate esters (PAEs), which are chemicals of high production volume and of toxicological concern (Xu et al., 2019; Zhao, 2019). PAEs are not chemically bonded to products and thus can be released into the environment inevitably (Cadogan et al., 1993; Xu et al., 2019). As the typical primary degradation product of PAEs, MPEs, have been widely detected in various aquatic environments (Suzuki et al., 2001; Jiang et al., 2018; Bartsch et al., 2019), such as seawater, groundwater and surface water, and even in human tissues

* Corresponding author.
E-mail: jwchen@dlut.edu.cn (J. Chen).

https://doi.org/10.1016/j.jes.2022.12.011
1001-0742/

and fluids (Hogberg et al., 2008), such as serum, liver, urine, breast milk. Health impairments due to the MPE exposure have been extensively reported, including endocrine disruption (Tian et al., 2019), hepatocarcinogenesis (David et al., 1999; Kaya et al., 2006), and reproductive and developmental toxicity (Sun et al., 2016). It is of significance to investigate the environmental behavior of MPEs for evaluating their persistence and ecological risk.

In comparison with the wide detections of MPEs in the environments, investigation on their environmental behavior and fate is still limited. With consideration of hydrolytic functional groups of carboxylic ester bonds in the MPEs, hydrolysis can be a crucial transformation pathway. In aqueous environments, for which pH is normally between 5 and 9, base-catalyzed (reaction with OH^-) and neutral (reaction with H_2O) hydrolysis are important (Schwarzenbach et al., 2003). Hydrolytic half-lives ($t_{1/2}$) of MPEs can be derived from the second-order rate constant for base-catalyzed hydrolysis (k_B) and the second-order constant for neutral hydrolysis (k_N). As key parameters for assessing the environmental persistence, k_B and k_N values are lacking for most MPEs. Therefore, it is necessary to determine k_B and k_N values of MPEs.

For chemicals that have the same main structural moieties (e.g., parabens (Ding et al., 2017; Xu et al., 2021), organophosphate triesters (Su et al., 2016), and PAEs (Xu et al., 2019)), structural variations in leaving group can significantly change their environmental behaviors and toxicological effects. For example, computational results in a previous study (Xu et al., 2019) showed that hydrolysis kinetics and rate-determining steps of the PAEs depend on the nature of leaving groups. However, how the base-catalyzed and neutral hydrolysis behavior of MPEs can be affected by their leaving groups remains unclear.

Hydrolytic behavior and kinetics of MPEs can be investigated by experiments and quantum chemical calculations. However, experimental determinations can be ambiguous, as different pathways or mechanisms may give rise to similar observations. Another important problem may exist in the experimental analysis for the MPE hydrolysis is the risk of contamination, since PAEs and their metabolites are ubiquitous in the environments and even in plastic materials used for analysis (Net et al., 2015). Quantum chemical methods, e.g., density functional theory (DFT), may overcome the limitations of the experimental determination (Blotevogel et al., 2011; Zhang et al., 2015; Gould, 2017; Szeler et al., 2020). In addition, the previous study has already indicated that DFT calculated results about hydrolysis of PAEs were consistent with the corresponding experimental results (Xu et al., 2019). Therefore, it is feasible to investigate MPE hydrolysis by the DFT calculation.

However, it is unpractical to calculate the k_B and k_N values for all MPEs only by DFT calculations due to their high computational costs, which indicates the necessity of developing high-throughput methods. Quantitative structure-activity relationship (QSAR) and linear free energy relationship (LFER) have been proven to be particularly useful for investigating hydrolysis kinetics for a series of compounds with similar structures (Schwarzenbach et al., 2003; Duarte et al., 2015, 2016). Based on LFER, Duarte et al. investigated the effects of leaving groups on the competition between solvent-assisted and substrate-assisted mechanisms for phosphate monoester dianion hydrolysis, and demonstrated that the mechanistic choice depends on the nature of the leaving groups (Duarte et al., 2016). Therefore, LFER and QSAR model can be employed to analyze the leaving group effects on the hydrolysis of MPEs and predict their hydrolysis kinetics parameters.

In this study, based on the appropriate DFT method that has been evaluated in our previous study (Xu et al., 2019), the kinetics of base-catalyzed and neutral hydrolysis for 18 MPEs with different leaving groups (Fig. 1) were investigated. The leaving group effects on the hydrolysis mechanisms and kinetics of MPEs were analyzed. Finally, a QSAR model that can be employed to predict k_B values of MPEs were developed, which promises to fill the data gap of hydrolysis kinetics for MPEs.

1. Computational details

1.1. *Model chemicals*

18 MPEs with various leaving groups were selected as model compounds (Fig. 1). 10 of them (i.e., mono-methyl, mono-ethyl, mono–butyl, mono-hexyl, mono-heptyl, mono-octyl, mono-2-ethylhexyl, mono-nonyl, mono-decyl and mono-benzyl phthalate (MMP, MEP, MBP, MHP, MC7P, MC8P, MEHP, MC9P, MC10P and MBzP)) are the MPEs that have been detected in the environment (Suzuki et al., 2001; Jiang et al., 2018). The alkyls in the leaving groups of these MPEs belong to electron donating groups. To explain the influence of electronic effects of the leaving groups on MPE hydrolysis, MPEs with electron withdrawing groups were designed, by taking mono-phenyl phthalate (MPhP) as a main structure, then adding different electron withdrawing groups on the phenyl in the leaving groups. The variety of geometries provides the possibility to investigate the influence of the steric hindrance and the electronic effects of the leaving groups on MPE hydrolysis, and develop the QSAR model. As the proton in the carboxylic acid ($pK_a = 3.32$, predicted by ACD Labs) is dissociated in the actual aquatic environment (pH = 5–9), MPE anions were adopted in following DFT calculations.

1.2. *Quantum chemical calculation*

Before calculating hydrolysis pathways and kinetics, it is necessary to identify the optimal conformations for the MPE anions, as their flexible side chains can result in various molecular conformations. The global minimum for each MPE was searched by *ab initio* molecular dynamics using TURBOMOLE program (Ahlrichs et al., 1989), as detailed in the Appendix A. The conformation with the lowest energy was adopted to investigate hydrolysis pathways and kinetics.

All DFT calculations were performed on Gaussian 09 program (Frisch et al., 2009). The B3LYP (Stephens et al., 1994) functional has been previously employed to study hydrolysis mechanisms and kinetics and shown good performance (Blotevogel et al., 2011; Zhang et al., 2015). The split-valence 6–311++G(2d,2p) basis set is commonly employed in studies about hydrolysis of chemicals (Hill et al., 2012; Xu et al.,

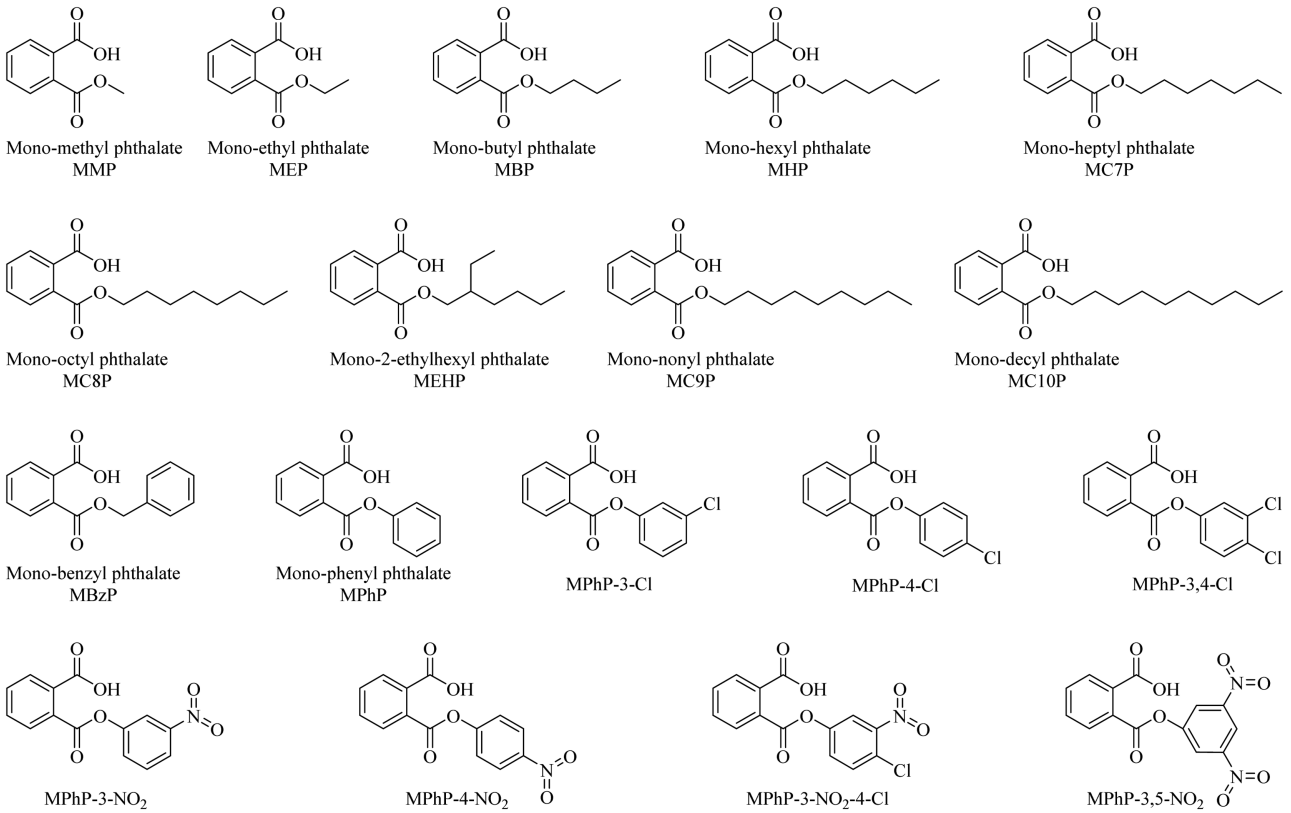

Fig. 1 – Molecular structures of MPEs in this study.

2019). The integral equation formalism of the polarized continuum model (IEFPCM) can be employed to simulate the aqueous environment (Tomasi et al., 2005). More importantly, a previous study has compared calculated k_B values by different DFT methods and solvation models with the corresponding experimental k_B values of PAEs, which has proven that IEFPCM/B3LYP/6–311++G(3df,2pd)//IEFPCM/B3LYP/6–311++G(2d,2p) can be employed to investigate base-catalyzed hydrolysis of PAEs (Xu et al., 2019).

Thus, conformations of reactants (R), reactive complexes (RC), transition states (TS), intermediates (IM) and products (P) of the base-catalyzed and neutral hydrolysis of the MPEs were optimized at the IEFPCM/B3LYP/6–311++G(2d,2p) level. Single point energies of these conformations were calculated at the IEFPCM/B3LYP/6–311++G(3df,2pd) level. Frequency analysis was conducted to ensure that TS has only one imaginary frequency, and other conformations only have real frequencies. Intrinsic reaction coordinate calculation was carried out to confirm that TS connects expected reactants and products.

Calculations of Hirshfeld atomic charge and Wiberg bond order for the MPEs were performed on Multiwfn software (Lu and Chen, 2012). pK_a values of parent compounds and hydrolysis products were predicted by a pK_a prediction module in MOPAC (Stewart, 2016) at PM6 level.

The Gibbs free energies of reaction (ΔG) for all the base-catalyzed and neutral hydrolysis pathways were calculated by the energy difference between R and P, and the Gibbs free energies of activation ($\Delta G^{\ddagger}$) were calculated as the energy difference between R and TS of the rate-determining step of the corresponding pathways. For all the reactions, the aqueous molar standard state was considered. Details for $\Delta G^{\ddagger}$ corrections are provided in the Appendix A.

Transition state theory was employed to calculate the k_B and k_N values of the MPEs:

$$k = \kappa_{rd} \cdot \left(\frac{k_b \cdot T}{h}\right) \cdot \exp\left(\frac{-\Delta G^{\ddagger}}{R \cdot T}\right) \quad (1)$$

where k ($sec^{-1}{\cdot}mol^{-1}{\cdot}L$) is k_B or k_N, κ_{rd} is the transmission coefficient, k_b (1.380×10^{-23} $J{\cdot}K^{-1}$) is the Boltzmann's constant, T (K) is the temperature and was set as 298.15 K, h (6.626×10^{-34} J·sec) is the Planck constant, and R (8.314 $J{\cdot}mol^{-1}{\cdot}K^{-1}$) is the molar gas constant.

1.3. QSAR modeling

A QSAR model was developed based on the DFT calculated k_B values of MPEs by stepwise multiple linear regression. 18 MPEs were randomly divided into training and validation sets with a ratio of 5:1. Molecular structural descriptors were calculated by Gaussian 09 and Dragon 6.0 (Talete, 2012) based on the optimized geometries at the IEFPCM/B3LYP/6–311++G(2d,2p) level. Different molecular descriptors can have different data ranges, which may influence the screen of descriptors. Therefore, values for all the descriptors were standardized to eliminate this influence, as detailed in the Appendix A. Williams

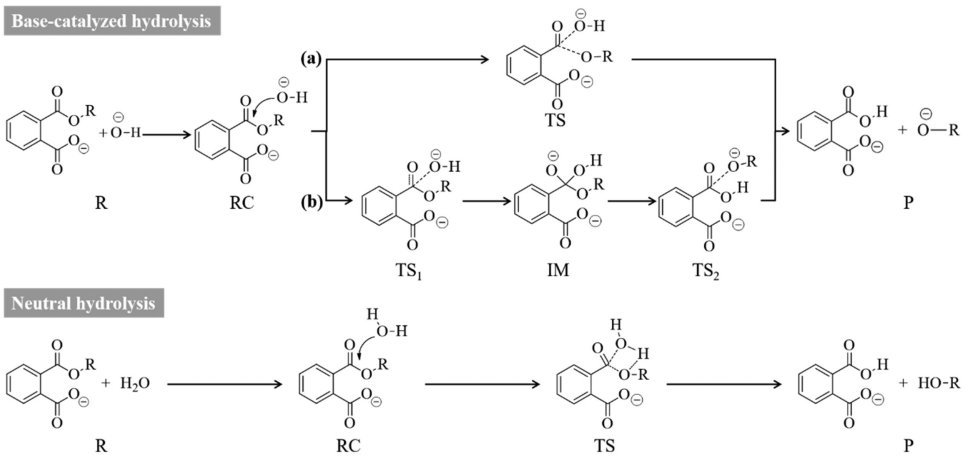

Fig. 2 – Schematic pathway of the base-catalyzed and neutral hydrolysis of MPE anions (The symbols R, RC, TS, IM and P represent reactants, pre-reaction complexes, transition states, intermediates and products, respectively.).

plot (Li et al., 2013) was employed to characterize the application domain.

2. Results and discussion

2.1. *Pathways of base-catalyzed and neutral hydrolysis*

As shown in Fig. 2, the MPEs undergo the base-catalyzed hydrolysis through two types of pathways: (a) an RC, a dissociative TS formed by the nucleophilic attack of OH^- on the C atom of the ester bond concerted with the departure of the leaving group, and finally leads to the corresponding acid and unprotonated leaving group ($R\text{-}O^-$); (b) an RC, a TS_1 formed by the nucleophilic attack of OH^- on the C atom of the ester bond, an IM, and a TS_2 formed by the partly departure of the leaving group from the ester bond, and finally generates the same products as the pathway (a). The neutral hydrolysis of the MPEs proceeds through an RC, a dissociative TS with a four-membered ring formed by the attack of H_2O on the ester bond (i.e., the O atom in the H_2O attacks the C atom in the ester bond, and the H atom in the H_2O and the O atom in the leaving group form a hydrogen bond), and finally leads to the acid and protonated leaving group (R-OH).

The mechanisms of the base-catalyzed hydrolysis that undergoes the pathway (a) and the neutral hydrolysis belong to S_N2 mechanism, where the nucleophiles (OH^- and H_2O) push the leaving groups out of the MPEs. The mechanism of the base-catalyzed hydrolysis that goes through pathway (b) belongs to S_N1 mechanism.

Free energy surfaces for MMP and MPhP are shown in Fig. 3, and for the others are shown in Appendix A Fig. S1. $\Delta G^{\ddagger}$ values of the rate-determining steps for the base-catalyzed and the neutral hydrolysis are shown in Appendix A Table S1. As shown in Fig. 3, the base-catalyzed hydrolysis follows the pathway (b) and the rate-determining step only depends on the nucleophilic attack of OH^- for MMP, which has a poor leaving group (i.e., methyl alcohol). For MPhP that has a good leaving group (i.e., phenol), the base-catalyzed hydrolysis follows the pathway (a) and the rate-determining step depends on the nucleophilic attack of OH^- and the departure of the leaving group. As shown in Appendix A Fig. S1, similar phenomena have been found for the other MPEs. It can thus be concluded that the choice between the two pathways depends on the nature of the leaving group, and the MPE with a good leaving group (i.e. group with pK_a of <10) prefers a dissociative TS.

It deserves mentioning that the base-catalyzed hydrolysis for the parent compounds of MPEs has two types of rate-determining steps. For some PAEs, the rate-determining step is the nucleophilic attack of OH^- on the C atom of the ester bonds. For the others, the rate-determining step is the departure of the leaving groups from the ester bonds. In contrast with that, the rate-determining step of the base-catalyzed hydrolysis for the MPEs is the nucleophilic attack of OH^-.

A QSAR model that can be employed to predict the rate-determining steps has been developed in the previous study about PAE hydrolysis (Xu et al., 2019). This model indicated that there are three factors determining the rate-determining step, including Hirshfeld atomic charge on the O atom of the leaving groups, energy of the highest occupied molecular orbital (E_{HOMO}) of the substructure, and aromaticity index of the target compounds. These three molecular descriptors were calculated for the MPEs (listed in Appendix A Table S2), and the rate-determining steps of the MPEs were predicted based on this model. All predicted rate-determining steps of the base-catalyzed hydrolysis for the MPEs were the nucleophilic attack of OH^-, which is consistent with the DFT calculation results in the present study. The three descriptors involved in the QSAR model describe electronic effects of structural moieties of target compounds. Therefore, it can be speculated that contribution of the electronic effects on energetic barrier is greater than that of the steric hindrance effects for the base-catalyzed hydrolysis of the PAEs and MPEs.

2.2. *Kinetics of base-catalyzed and neutral hydrolysis*

As can be seen from Fig. 3 and Appendix A Fig. S1, ΔG values of the neutral hydrolysis are greater than 0 for MMP, MEP, MBP, MHP, MC7P, MC8P, MEHP, MC9P, MC10P and MBzP, which indicates that the neutral hydrolysis for these MPEs is not

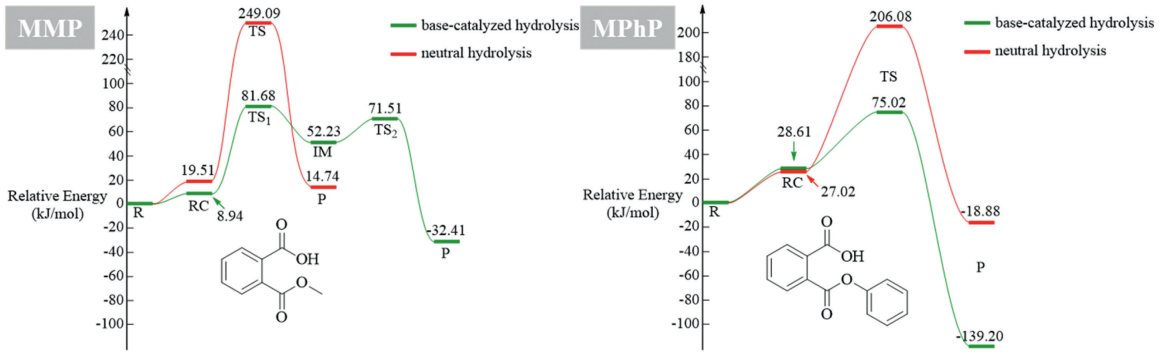

Fig. 3 – Schematic free-energy surfaces for the base-catalyzed and the neutral hydrolysis of MMP and MPhP (The total energy of the reactants and nucleophiles (OH^- or H_2O) is set to zero (reference state). The symbols R, RC, TS, IM, and P represent reactants, prereactive complexes, transition states, intermediates and products, respectively.).

Table 1 – DFT calculated k_B ($mol^{-1}\cdot L\cdot sec^{-1}$) and k_N ($mol^{-1}\cdot L\cdot sec^{-1}$) values for MPEs at the IEFPCM/B3LYP/6–311++G(3df,2pd)//IEFPCM/B3LYP/6–311++G(2d,2p) level.

MPEs	k_B	MPEs	k_B	k_N
MMP	3.11×10^{-2}	MBzP	2.52×10^{-2}	–
MEP	1.20×10^{-2}	MPhP	4.58×10^{-1}	5.18×10^{-24}
MBP	7.93×10^{-3}	MPhP-3-Cl	3.84×10^{1}	1.29×10^{-21}
MHP	2.64×10^{-2}	MPhP-4-Cl	1.97×10^{-1}	6.91×10^{-23}
MC7P	2.36×10^{-2}	MPhP-3,4-Cl	8.74×10^{0}	5.61×10^{-21}
MC8P	7.62×10^{-3}	MPhP-3-NO_2	2.89×10^{1}	9.26×10^{-21}
MEHP	2.78×10^{-3}	MPhP-4-NO_2	1.64×10^{0}	7.21×10^{-25}
MC9P	6.13×10^{-3}	MPhP-3-NO_2–4-Cl	2.74×10^{1}	5.18×10^{-24}
MC10P	1.79×10^{-2}	MPhP-3,5-NO_2	3.40×10^{2}	3.92×10^{-23}

thermodynamically feasible. Therefore, the k_N values of these MPEs were not calculated. DFT calculated k_B of 18 MPEs and k_N values of a part of MPEs in the present study are listed in Table 1.

Although water molecules ($[H_2O] = 55.56\ mol\cdot L^{-1}$) are abundant enough for MPEs in aqueous environment to undergo the neutral hydrolysis, the energetic barrier of the neutral hydrolysis is much higher than that of the base-catalyzed hydrolysis (Appendix A Table S1). Therefore, it is obvious that reaction with OH^- (base-catalyzed hydrolysis) is also predominant at neutral conditions and even at conditions of pH lower than 7. Based on the k_B and k_N values, $t_{1/2}$ of MPEs at different pH conditions were calculated and are listed in Appendix A Table S3. At pH = 7, the $t_{1/2}$ values range from 5.67 hr (MPhP-3,5-NO_2) to 79.2 years (MEHP). At pH = 9, the $t_{1/2}$ values range from 3.4 min to 289 days. From the $t_{1/2}$ values of the substituted MPhP by different substituents, it can be seen that the $t_{1/2}$ of MPEs can be shortened by adding electron withdrawing groups on the leaving-groups.

A QSAR model that can be employed to predict the k_B values for the PAEs with the nucleophilic attack of OH^- as the rate-determining step has been developed in the previous study (Xu et al., 2019), which indicates the k_B values are significantly related to polarizability (α) of target compounds. The α values of the MPEs were calculated and listed in Appendix A Table S4. However, QSAR-predicted k_B values are far from the DFT-calculated k_B values for the MPEs, which further indicates the necessity of developing prediction models for the k_B of the MPEs.

2.3. *Substituent effects on pK_a of leaving groups and hydrolysis kinetics of MPhP*

The pK_a values of the leaving groups were listed in Appendix A Table S5, some were adopted from literature (Duarte et al., 2016), and the others were calculated by a pK_a prediction module on MOPAC software (Stewart, 2016) at PM6 level.

The electronic and steric effects of different substituents on pK_a of the leaving groups, $\log k_B$ and $\log k_N$ of MPhP were investigated. As listed in Table 2, the -Cl substituent decreased the pK_a of MPhP by 0.98 (*meta*-position) and 0.62 (*para*-position) pK_a units. The –NO_2 substituent decreased the pK_a of MPhP by 1.65 (*meta*-position) and 2.86 (*para*-position) pK_a units. Comparison between *meta*- and *para*-substitution of –Cl and –NO_2 groups, indicates that proximity effect of –Cl decreases the pK_a of the leaving group of MPhP, and proximity effect of –NO_2 increases that. It can also be found that the –NO_2 substituent shows larger negative inductive effects on the pK_a of leaving group of MPhP than the –Cl substituent.

As shown in Table 2, the negative inductivity of the –NO_2 and –Cl substituents enhanced the base-catalyzed and neutral hydrolysis of MPhP. However, the –NO_2 substituent does not show obviously greater enhancement on $\log k_B$ and $\log k_N$

Table 2 – Effects of substituents on pK_a and hydrolysis kinetics.

MPEs	ΔpK_a[a]	$\Delta \log k_B$[b]	$\Delta \log k_N$[c]
MPhP	0	0	0
MPhP-3-Cl	−0.98	1.92	2.40
MPhP-4-Cl	−0.62	−0.367	1.13
MPhP-3,4-Cl	−1.37	1.28	3.03
MPhP-3-NO_2	−1.65	1.80	3.25
MPhP-4-NO_2	−2.86	0.554	−0.856
MPhP-3-NO_2–4-Cl	−2.22	1.78	3.70
MPhP-3,5-NO_2	−3.32	2.87	0.879

[a] ΔpK_a was calculated by the difference between pK_a of substituted MPhP and pK_a of MPhP ($\Delta pK_a = pK_{a-MPE} - pK_{a-MPhP}$).
[b] $\Delta \log k_B$ was calculated by the difference between $\log k_B$ of substituted MPhP and $\log k_B$ of MPhP ($\Delta \log k_B = \log k_{B-MPE} - \log k_{B-MPhP}$).
[c] $\Delta \log k_N$ was calculated by the difference between $\log k_N$ of substituted MPhP and $\log k_N$ of MPhP ($\Delta \log k_N = \log k_{N-MPE} - \log k_{N-MPhP}$).

than the –Cl substituent. It is possibly due to the larger steric hindrance of the –NO_2 group than that of the –Cl atom.

2.4. Leaving group effects on hydrolysis kinetics

As shown in Appendix A Fig. S2, the $\log k_B$ values are in linear relationships with pK_a values of the leaving groups for the MPEs, and the regression coefficient is 0.928. The larger is the pK_a of the leaving groups, the smaller are the k_B values of the MPEs. This linear relationship can be expressed in the form of the Brönsted relationship as follows:

$$\log k_B = -2.34\,pK_a + 11.2 \quad (2)$$

pK_a can reflect the electron withdrawing ability of the leaving groups and the difficulty of the dissociation of the leaving groups from the ester bonds. The easier is the dissociation of the leaving group, the lower is the enegetic barrier of MPE hydrolysis, and thus the faster is the hydrolysis kinetics.

The Brönsted relationship has been reported for carbamates and organophosphate esters, which correlates $\log k_B$ with pK_a of leaving groups (Kirby and Varvogli, 1967; Lad et al., 2003; Schwarzenbach et al., 2003; Bartsch et al., 2019). Previous studies indicated that the high sensitivity of the hydrolysis rate to pK_a of leaving groups can be interpreted as resulting from a loose TS with extensive bond cleavage to the leaving group (Duarte et al., 2016). Also, in the conditions where LFERs can correlate $\log k_B$ with pK_a of leaving groups, the departure of the leaving groups is the rate-determining step (Schwarzenbach et al., 2003). However, the rate-determining step is the nucleophilic attack of OH^- for all the MPEs in the present study. There should be other factors (See the section of QSAR modeling) determining the hydrolysis kinetics of MPEs.

Among the 18 MPEs in this study, 8 MPEs are taking MPhP as the main structure and substituted by different electron withdrawing groups on their leaving groups; 7 MPEs have linear alkyl in their side chains; 1 MPEs (MEHP) has branched alkyl in its side chains; and the last one is MBzP with benzyl in side chains. The investigation in this study unveils that the 8 MPEs with MPhP as basic moiety are the most vulnerable to undergo base-catalyzed and neutral hydrolysis. Although MEHP and MC8P contain the same amount of C atoms, hydrolysis of MEHP with branched alkyl side chain is slower than that of MC8P with linear alkyl side chain.

2.5. Leaving group effects on TS geometries

As shown in Appendix A Fig. S3, TS (TS in the pathway (a) and TS_2 in the pathway (b) showin in Fig. 2) geometries of the base-catalyzed hydrolysis for the MPEs varied as a function of pK_a of the leaving groups. The stronger is the electron withdrawing ability of the leaving group, the smaller is the bond order between C atom in the ester bond and O atom in the leaving group (O_{lg}). It is reasonable that the smaller is the pK_a of the leaving group, the easier is the dissociation of C–O_{lg} covalent bond, leading to the looser is the TS geometry. Information on the nature of the TS of MPE hydrolysis is an important building block to well understand the enzyme-involved reactions of these endocrine disrupting chemicals in the biological system.

2.6. QSAR modeling

Since the sample size of k_N values for the MPEs is limited and the neutral hydrolysis can be neglected in the actual environment, model for predicting k_N values was not developed. Based on the DFT calculated k_B values of the 18 MPEs, a QSAR model that can be employed to predict k_B for more MPEs was developed as follows:

$$\log k_B = -3.39\,pK_a + 0.44\chi + 1.20$$
$$n_{tra} = 15,\ R^2_{tra} = 0.854,\ Q^2_{LOO} = 0.728,$$
$$n_{ext} = 3,\ R^2_{ext} = 0.988,\ Q^2_{ext} = 0.943 \quad (3)$$

where χ is the electronegativity of MPEs [$\chi = -(E_{HOMO} + E_{LUMO})/2$, where E_{HOMO} is the energy of the highest occupied molecular orbital, E_{LUMO} is the energy of the lowest unoccupied molecular orbital]; n_{tra} and n_{ext} represent the number of MPEs in the training and validation sets, respectively; R^2 stands for the determination coefficient; Q^2_{LOO} represents the leave-one-out cross-validated determination coefficient; and Q^2_{ext} represents the external validation coefficient.

The statistical parameter values indicate the QSAR model has good goodness-of-fit, robustness, and predictive ability. The variable inflation factor (*VIF*) is 2.28 for both pK_a and χ, which is much smaller than 5. Thus, the model is free of multicollinearity (O'Brien, 2007). The difference between R^2 and Q^2 is smaller than 0.3, indicating that the model is free of overfitting (Golbraikh and Tropsha, 2002). As shown in Fig. 4A, the QSAR predicted $\log k_B$ values are consistent with the DFT calculated $\log k_B$ values. The application domain was characterized by Williams plot, which is based on standardized residual (δ) and leverage (h). Calculation details about the δ and h values are described in the Appendix A. As shown in Fig. 4B, the absolute values of δ are smaller than 3, and the h values are smaller than the warning value ($h^* = 0.600$), which indicates that there is no outlier in this model. Thus, the developed QSAR model can be employed to predict the k_B values of other MPEs in the application domain.

As discussed in section of leaving group effects on hydrolysis kinetics, it is not surprising that the pK_a of the

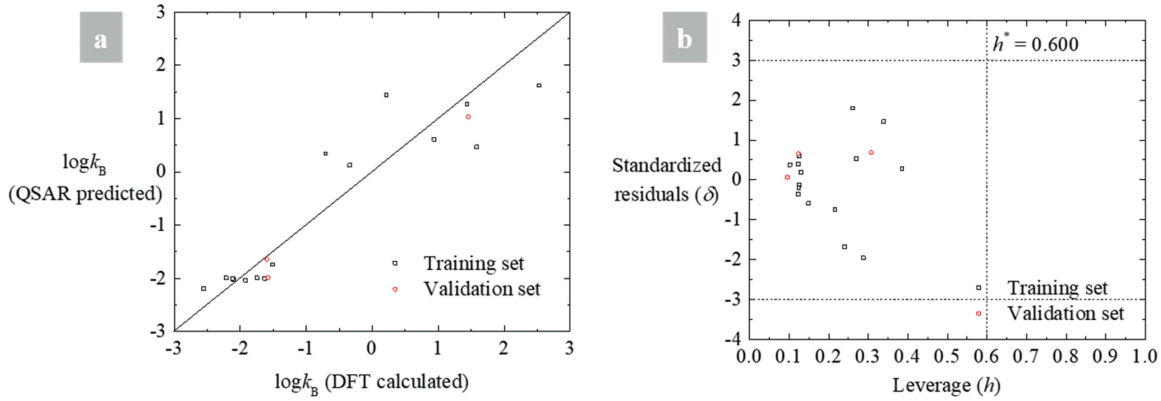

Fig. 4 – a. Plot for the QSAR model predicted logk_B values versus the DFT calculated logk_B values; b. Williams plot indicating the application domain of the QSAR model.

leaving group is the most important molecular descriptor in this model. Another factor determining hydrolysis kinetics of MPEs, is the electronegativity of MPEs. Electronegativity is the negative of chemical potential, which reflects the reactivity of chemicals (Chattaraj et al., 2011). The larger is the χ value, the more reactive is the MPEs, and thus the larger is the logk_B of MPEs.

3. Conclusion

For assessing the environmental persistence and ecological risk of PAEs, the chemicals of high production volume and of toxicological concern, it is indispensable to understand the environmental behavior of MPEs. In this study, leaving group effects on hydrolysis pathways and kinetics for the MPEs have been explored. Results indicate pK_a of the leaving groups and the hydrolysis kinetics of MPEs show a significant linear relationship. The smaller is the pK_a value of the leaving group, the faster is the base-catalyzed hydrolysis of MPEs. Futhermore, a QSAR model that can be employed to predict the base-catalyzed hydrolysis kinetics for the MPEs was developed. It is worth exploring the influences of other environmental factors in the future studies, such as mineral (e.g., goethite, kaolinite) adsorption, for better understanding the transformation process that governs the environmental fate of PAEs and MPEs.

Declaration of Competing Interest

The authors declare that they have no known competing financial interests or personal relationships that could have appeared to influence the work reported in this article.

Acknowledgments

This study was supported by the National Natural Science Foundation of China (No. 22136001), the National Key R&D Program of China (No. 2022YFC3902100), the Key R&D Program of Hebei Province (No. 21374001D), the Supercomputing Center of Dalian University of Technology, and the National Supercomputer Center in Tianjin.

Appendix A Supplementary data

Supplementary material associated with this article can be found, in the online version, at doi:10.1016/j.jes.2022.12.011.

REFERENCES

Ahlrichs, R., Bar, M., Haser, M., Horn, H., Kolmel, C., 1989. Electronic-structure calculations on workstation computers - the program system Turbomole. Chem. Phys. Lett. 162, 165–169.

Bartsch, P.W., Edwards, T.M., Brock, J.W., 2019. Prevalence of eight phthalate monoestersin water from the Okavango Delta, Northern Botswana. Bull. Environ. Contam. Toxicol. 103 (2), 274–279.

Blotevogel, J., Mayeno, A.N., Sale, T.C., Borch, T., 2011. Prediction of contaminant persistence in aqueous phase: a quantum chemical approach. Environ. Sci. Technol. 45, 2236–2242.

Cadogan, D.F., Papez, M., Popp¢, A.C., Scheubel, J., 1993. An assessment of the release, occurrence and possible effect of plasticizers in the environment. Prog. Rubber Plast. Technol. 10, 1–19.

Chattaraj, P.K., Giri, S., Duley, S., 2011. Update 2 of: electrophilicity index. Chem. Rev. 111, PR43–PR75.

David, R.M., Moore, M.R., Cifone, M.A., Finney, D.C., Guest, D., 1999. Chronic peroxisome proliferation and hepatomegaly associated with the hepatocellular tumorigenesis of di(2-ethylhexyl)phthalate and the effects of recovery. Toxicol. Sci. 50, 195–205.

Ding, K.K., Kong, X.T., Wang, J.P., Lu, L.P., Zhou, W.F., Zhan, T.J., et al., 2017. Side chains of parabens modulate antiandrogenic activity: *in vitro* and molecular docking studies. Environ. Sci. Technol. 51, 6452–6460.

Duarte, F., Aqvist, J., Wiliams, N.H., Kamerlin, S.C.L., 2015. Resolving apparent conflicts between theoretical and experimental models of phosphate monoester hydrolysis. J. Am. Chem. Soc. 137, 1081–1093.

Duarte, F., Barrozo, A., Aqvist, J., Williams, N.H., Kamerlin, S.C.L., 2016. The competing mechanisms of phosphate monoester dianion hydrolysis. J. Am. Chem. Soc. 138, 10664–10673.

Frisch, M.J., Trucks, G.W., Schlegel, H.B., Scuseria, G.E., Robb, M.A., Cheeseman, J.R., et al., 2009. Gaussian 09, Revision A.01. Gaussian, Inc., Wallingford CT.

Golbraikh, A., Tropsha, A., 2002. Beware of q^2!. J. Mol. Graph. Model 20, 269–276.

Gould, T., 2017. What makes a density functional approximation good? Insights from the left Fukui function. J. Chem. Theory Comput. 13, 2373–2377.

Hill, F.C., Sviatenko, L.K., Gorb, L., Okovytyy, S.I., Blaustein, G.S., Leszczynski, J., 2012. DFT M06-2X investigation of alkaline hydrolysis of nitroaromatic compounds. Chemosphere 88, 635–643.

Hogberg, J., Hanberg, A., Berglund, M., Skerfving, S., Remberger, M., Calafat, A.M., et al., 2008. Phthalate diesters and their metabolites in human breast milk, blood or serum, and urine as biomarkers of exposure in vulnerable populations. Environ. Health Persp. 116, 334–339.

Jiang, J.Q., Mu, D., Ding, M.Y., Zhang, S.Y., Zhang, H., Hu, J.Y., 2018. Simultaneous determination of primary and secondary phthalate monoesters in the Taihu Lake: exploration of sources. Chemosphere 202, 17–24.

Kaya, T., Mohr, S.C., Waxman, D.J., Vajda, S., 2006. Computational screening of phthalate monoesters for binding to PPAR gamma. Chem. Res. Toxicol. 19, 999–1009.

Kirby, A.J., Varvogli, A., 1967. Reactivity of phosphate esters. Monoester hydrolysis. J. Am. Chem. Soc. 89, 415.

Lad, C., Williams, N.H., Wolfenden, R., 2003. The rate of hydrolysis of phosphomonoester dianions and the exceptional catalytic proficiencies of protein and inositol phosphatases. Proc. Natl. Acad. Sci. U.S.A. 100, 5607–5610.

Li, X.H., Zhao, W.X., Li, J., Jiang, J.Q., Chen, J.J., Chen, J.W., 2013. Development of a model for predicting reaction rate constants of organic chemicals with ozone at different temperatures. Chemosphere 92, 1029–1034.

Lu, T., Chen, F.W., 2012. Multiwfn: a multifunctional wavefunction analyzer. J. Comput. Chem. 33, 580–592.

Net, S., Sempere, R., Delmont, A., Paluselli, A., Ouddane, B., 2015. Occurrence, fate, behavior and ecotoxicological state of phthalates in different environmental matrices. Environ. Sci. Technol. 49, 4019–4035.

O'Brien, R.M., 2007. A caution regarding rules of thumb for variance inflation factors. Qual. Quant. 41, 673–690.

Schwarzenbach, R.P., Gschwend, P.M., Imboden, D.M., 2003. Environmental Organic Chemistry, 2nd ed. John Wiley & Sons, Hoboken, NJ.

Talete s.r.l., 2012. DRAGON (Software for Molecular Descriptor Calculation) Version 6.0.

Stephens, P.J., Devlin, F.J., Chabalowski, C.F., Frisch, M.J., 1994. *Ab initio* calculation of vibrational absorption and circular-dichroism spectra using density-functional force-fields. J. Phys. Chem. US 98, 11623–11627.

Stewart, J.J.P., 2016. MOPAC 2016. Stewart Computational Chemistry, Colorado Springs, CO, USA.

Su, G.Y., Letcher, R.J., Yu, H.X., 2016. Organophosphate flame retardants and plasticizers in aqueous solution: pH-dependent hydrolysis, kinetics, and pathways. Environ. Sci. Technol. 50, 8103–8111.

Sun, J., Zhang, M.R., Zhang, L.Q., Zhao, D., Li, S.G., Chen, B., 2016. Phthalate monoesters in association with uterine leiomyomata in Shanghai. Int. J. Environ. Health Res. 26, 306–316.

Suzuki, T., Yaguchi, K., Suzuki, S., Suga, T., 2001. Monitoring of phthalic acid monoesters in river water by solid-phase extraction and GC–MS determination. Environ. Sci. Technol. 35, 3757–3763.

Szeler, K., Williams, N.H., Hengge, A.C., Kamerlin, S.C.L., 2020. Modeling the alkaline hydrolysis of diaryl sulfate diesters: a mechanistic study. J. Org. Chem. 85, 6489–6497.

Tian, M.P., Zhang, X., Liu, L.P., Martin, F.L., Wang, H., Zhang, J., et al., 2019. Phthalate side-chain structures and hydrolysis metabolism associated with steroidogenic effects in MLTC-1 Leydig cells. Toxicol. Lett. 308, 56–64.

Tomasi, J., Mennucci, B., Cammi, R., 2005. Quantum mechanical continuum solvation models. Chem. Rev. 105, 2999–3093.

Xu, T., Chen, J.W., Wang, Z.Y., Tang, W.H., Xia, D.M., Fu, Z.Q., et al., 2019. Development of prediction models on base-catalyzed hydrolysis kinetics of phthalate esters with density functional theory calculation. Environ. Sci. Technol. 53, 5828–5837.

Xu, T., Chen, J.W., Chen, X., Xie, H.J., Wang, Z.Y., Xia, D.M., et al., 2021. Prediction models on pK_a and base-catalyzed hydrolysis kinetics of parabens: experimental and quantum chemical studies. Environ. Sci. Technol. 55, 6022–6031.

Zhang, H.Q., Xie, H.B., Chen, J.W., Zhang, S.S., 2015. Prediction of hydrolysis pathways and kinetics for antibiotics under environmental pH conditions: a quantum chemical study on cephradine. Environ. Sci. Technol. 49, 1552–1558.

Zhao, H.Y., 2019. Occurrence of phthalate monoesters in environment: a mini-review. IOP Conf. Ser: Earth Environ. Sci. 233, 042005.